Synthesis of a Multinanoparticle-Embedded Core/Mesoporous Silica Shell Structure As a Durable Heterogeneous Catalyst

ARTICLE *in* LANGMUIR · MARCH 2012

Impact Factor: 4.46 · DOI: 10.1021/la2045898 · Source: PubMed

8 AUTHORS, INCLUDING:

Jianlin Shi
Chinese Academy of Sciences
459 PUBLICATIONS **13,621** CITATIONS
SEE PROFILE

Qianjun He
69 PUBLICATIONS **3,243** CITATIONS
SEE PROFILE

Feng Chen
37 PUBLICATIONS **1,542** CITATIONS
SEE PROFILE

Yu Chen
China University of Petroleum
425 PUBLICATIONS **7,264** CITATIONS
SEE PROFILE

Langmuir

Letter

pubs.acs.org/Langmuir

Synthesis of a Multinanoparticle-Embedded Core/Mesoporous Silica Shell Structure As a Durable Heterogeneous Catalyst

Lijun Wang, Jianlin Shi,* Yan Zhu, Qianjun He, Huaiyong Xing, Jian Zhou, Feng Chen, and Yu Chen

State Laboratory of High Performance Ceramic and Superfine Microstructure, Shanghai Institute of Ceramics, Chinese Academy of Sciences, Shanghai 200050, China

Supporting Information

ABSTRACT: A multi-nanoparticle-embedded amorphous aluminum/magnesium oxides (AAMO) core/mesoporous silica ($mSiO_2$) shell structure has been successfully synthesized by calcining the presynthesized catalyst precursor-containing layered double hydroxide (LDH) core/mesoporous silica shell composite. The well-dispersed catalytic nanoparticles were fixed at the interface between AAMO core and mesoporous SiO_2 shell, i.e., at the inner pore mouths of the mesoporous SiO_2 shell, which could effectively prevent nanoparticles from growth and/or aggregation with each other and in the meantime allow efficient access of reactants to the catalytic NPs. The final core/shell composite was found to be an efficient and highly recyclable heterogeneous catalyst.

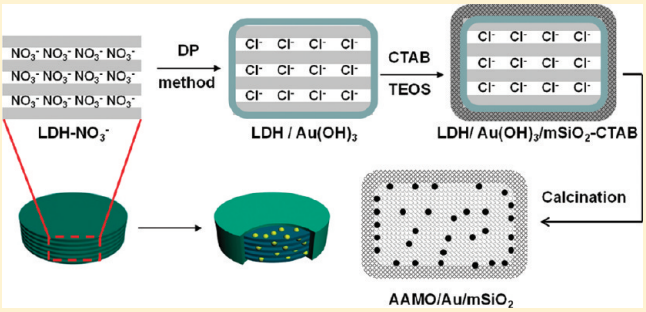

INTRODUCTION

Catalytic nanoparticles (NPs) have been extensively studied due to their unique properties compared to their bulk forms, leading to highly enhanced catalytic activity for various kinds of reactions.[1,2] Nanoparticles are, however, often subject to difficulties in handling and separation from reaction systems and, more importantly, irreversible deactivation in catalysis by the agglomeration among nanoparticles due to their overly high surface energy.[3,4] In order to resolve the problem, catalytic nanoparticles are usually coated with a layer of organic or inorganic capping agents, such as surfactants,[5] polymers,[6] metal oxides,[7,8] and carbon,[9] to stabilize them, or catalytic NPs can be loaded/dispersed in the mesoporous network of mesoporous hosts[10−12] for repeated catalytic activation.

Recently, the encapsulation of catalytic NPs as a core inside a porous inorganic shell has been paid much attention, because a porous inorganic shell can prevent nanoparticles from agglomerating with each other, meanwhile providing pathways for easy access of reactants to catalysts.[13−22] Generally, the catalytic NP core/porous inorganic shell-structured catalysts were prepared by coating a layer of porous inorganic shell on the surface of each as-synthesized catalytic NP.[8,9,17,18,23−25] This strategy suffers from the following drawbacks: (1) If the catalytic NP is small enough, e.g., several nanometers in diameter, a uniform, thin shell coating is usually not easy, and the coated NPs are still too small to handle. (2) If the coating is thick enough, the catalytic efficiency, as can be evaluated by TON value, becomes much lower. Therefore, researchers hope to encapsulate a number of NPs into one porous inorganic shell.[26−28] Unfortunately, the nanosized multiNPs in one core are subject to easy aggregation with each other during synthesis and/or employment. As expected, reports on the successful synthesis of the core/shell structure with a multinanoparticle-embedded core and outer mesoporous shell are few.[26−28]

Layered double hydroxides (LDHs), consisting of stacked brucite-type octahedral layers with anions and water molecules occupying the interlayer space, are currently attracting intense research interest.[29−34] As are the surfaces of the interlayers, the outer surface of the LDHs is positively charged and has abundant hydroxyl groups. Therefore, it can adsorb precursor anions of catalytic NPs, such as $[AuCl_4]^-$, $[PtCl_6]^{2-}$, $[PdCl_6]^{2-}$, $[IrCl_6]^{3-}$, and $[RuCl_6]^{3-}$,[35−37] or precursor of NPs, such as $Au(OH)_3$,[38] and even Fe_3O_4 NPs[39] without further chemical or physical modification. Taking advantage of this, here we propose that LDH particles with the precursor of NPs deposited on them be used as a core, i.e., hard template, in the meantime, to construct a core/shell structure by coating a mesoporous silica layer as the porous shell on the surface of the core. The catalytic NPs can be prepared on the core surface by the reduction/decomposition of precursor into metal NPs at a high temperature, and meanwhile, the template CTAB was removed from the mesoporous silica layer leaving penetrable mesopore channels in the shell. In this report, we demonstrate the synthesis of AAMO/Au core/$mSiO_2$ shell composite with the Au NPs fixed at the inner pore mouths of the mesoporous silica shell, which can be used as an efficient and highly durable heterogeneous catalyst. This method is expected to prepare

Received: January 16, 2012
Revised: February 28, 2012
Published: February 29, 2012

   dx.doi.org/10.1021/la2045898 | Langmuir 2012, 28, 4920−4925

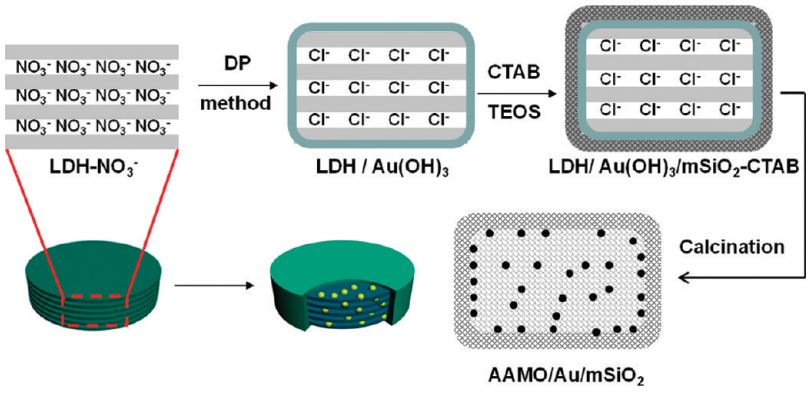

Figure 1. Schematic illustration for the synthesis of AAMO/Au/$mSiO_2$ composite.

other similar core/shell structured catalytic systems with highly dispersed multiple catalytic nanoparticles in the core part.

EXPERIMENTAL METHODS

Preparation of LDH-NO_3^{2-}. LDH-CO_3^{2-} was synthesized according to the literature[40] with a lower concentration of metal salt ions. Briefly, a mixed solution of $Mg(NO_3)_2{\cdot}6H_2O$ (0.016 M) and $Al(NO_3)_3{\cdot}9H_2O$ (0.008 M) was titrated with NaOH/$NaHCO_3$ (0.5 M/0.5 M) mixed solution at 25 °C. The final pH value of the solution was adjusted to 9.5 in 5 min, followed by hydrothermal treatment at 150 °C for 24 h. The obtained product was collected by centrifugation, washed with deionized water 3 times, and vacuum-dried. 65 mg LDH-CO_3^{2-} was further treated with 100 mL of aqueous solution containing $NaNO_3$ (0.75 mol) and HNO_3 (0.0025 mol) to expel interlayer carbonate ions for 1 day at ambient temperature. The sample LDH-NO_3^{2-} was recovered by centrifugation, washed with deionized water, and vacuum-dried.

Synthesis of LDH/Au(OH)$_3$. LDH-NO_3^- obtained was dissolved in 15 mL $HAuCl_4$ solution (2%) and the pH was adjusted to 8.0 quickly with NaOH solution. The solution was stirred at 60 °C in N_2 atmosphere for 24 h with the pH kept at 8.0. LDH/$Au(OH)_3$ was obtained by centrifugation, washing with deionized water, and vacuum-dried.

Synthesis of AAMO/Au/$mSiO_2$. LDH/$Au(OH)_3$ obtained as described above and 500 mg of cetyltrimethyl ammonium bromide (CTAB) were first mixed in deionized H_2O by ultrasonication for 30 min. The resultant homogeneous dispersion was diluted with 400 mL of deionized H_2O and 50 mL of NaOH aqueous solution (0.01 M) in a flask and further ultrasonically treated for 5 min. Afterward, the obtained basic dispersion was heated at 60 °C for 30 min under mechanical stirring to form a stable dispersion. Subsequently, 2.5 mL of tetraethylorthosilicate (TEOS)/ethanol (v/v:1/4) solution was injected into the stable dispersion, and the dispersion was further rapidly stirred for about 1 min and left standing for 12 h.[41,42] After the coating process, the product LDH/$Au(OH)_3$/$mSiO_2$−CTAB was collected by centrifugation, washed with ethanol at least 3 times, and vacuum-dried. AAMO/Au/$mSiO_2$ was obtained by calcining LDH/$Au(OH)_3$/$mSiO_2$−CTAB at 823 K for 6 h at the heating rate of 1 °C/min.

Synthesis of AAMO/Pt/$mSiO_2$ and AAMO/Au. The synthesis process of AAMO/Pt/$mSiO_2$ is the same as AAMO/Au/$mSiO_2$ using K_2PtCl_6 (40 mL, 0.5%) instead of $HAuCl_4$ (15 mL, 2%) with a solution pH of 7.2−7.6. After the coating process, LDH/Pt/$mSiO_2$ was obtained by calcining LDH/$[PtCl_4(H_2O)_2]$ /$mSiO_2$−CTAB, at 773 K in H_2 and N_2 mixed gases (5% H_2 + 95% N_2) for 2 h and then at 823 K in air for 4 h. AAMO/Au was obtained by calcining LDH/$Au(OH)_3$ at 773 K for 4 h.

Catalytic Reduction of 2-Nitroaniline. AAMO/Au/$mSiO_2$ (2.0 mg) was added to an excess amount of $NaBH_4$ aqueous solution (0.1 M). The mixture was ultrasonically stirred for 10 min at room temperature. Ten milliliters of 2-nitroaniline aqueous solution (6×10^{-3} M) was added, and the resulting mixture was stirred until the yellow solution became colorless. The reaction progress was monitored by taking a small portion of the reaction mixture every 5 min for each reaction. For 6 successive cycles of catalytic reduction of 2-nitroaniline, AAMO/Au/$mSiO_2$ (2.0 mg), AAMO/Au (2.0 mg) with a higher Au content than the former, and 2 mL 2-nitroaniline aqueous solution (6×10^{-3} M) were adopted. The reaction progress was monitored by taking a small portion of the reaction mixture after 15 min for each cycle. The conversion of 2-nitroaniline in each cycle was calculated based on the standard curve determined by UV−vis absorbance of 2-nitroaniline standard solutions.

Characterization. Transmission electron microscopy (TEM) images were obtained on a JEM-2100F electron microscope operating at an accelerating voltage of 200 kV. Scanning electron microscopy (SEM) images were obtained on S4800 field-emission scanning electron microscope. X-ray diffraction (XRD) pattern was collected using a Rigaku D/Max-2200 PC X-ray diffractometer with Cu target (40 kV, 40 mA). The UV/vis absorbance spectra were measured with a Shimadzu UV-3101PC spectrophotometer. Chemical composition analysis was performed with Varian Vista AX ICP-AES spectrometer. N_2 adsorption−desorption isotherms were obtained on a Micromeritics ASAP 3020 pore analyzer at 77 K under continuous adsorption conditions.

RESULTS AND DISCUSSION

Figure 1 schematically demonstrates the synthetic procedure of AAMO/Au/$mSiO_2$ composite. First, submicrometer-sized LDH-NO_3^{2-}, which consisted of positively charged hydroxide layers $(Mg^{2+}_{1-x}Al^{3+}_x(OH)_2)^{x+}$ with NO_3^{2-} anions intercalated in between these layers, which was more favorable to adsorb free precursor anions, such as $AuCl_4^-$, than CO_3^{2-},[43] was prepared by anion exchange of LDH-CO_3^{2-} with NO_3^-. Subsequently, the precursor of catalytic NPs, $Au(OH)_3$, was deposited on the surface of LDH-NO_3^- by mixing LDH-NO_3^- with $HAuCl_4$ at the pH value of 8.0, and this pH value is also most frequently selected in the deposition-precipitation (DP) method for the catalyst preparation of Au NPs when using $HAuCl_4$ as the precursor.[44,45] The obtained LDH/$Au(OH)_3$ composite was then coated with a layer of mesoporous silica by a self-assembly process between silicon precursor (TEOS) and surfactant CTAB under alkaline condition. Finally, by calcining LDH/$Au(OH)_3$/$mSiO_2$−CTAB intermediate at 550 °C, the final target product, AAMO/Au/$mSiO_2$ composite, was obtained, and in this process, $Au(OH)_3$ was converted to Au NPs, LDH decomposed into AAMO, and CTAB was removed leaving penetrable mesopore channels in the shell.

Figures 2a and S1 show the fabricated disk-like LDH-CO_3^{2-} with an average lateral dimension of about 250 nm and aspect ratio range from 4 to 8. The XRD pattern (Figure 3a) is typical of layer-structured $Mg_2Al(OH)_6(CO_3)_{0.5}$−LDH with the (001)

dx.doi.org/10.1021/la2045898 | Langmuir 2012, 28, 4920−4925

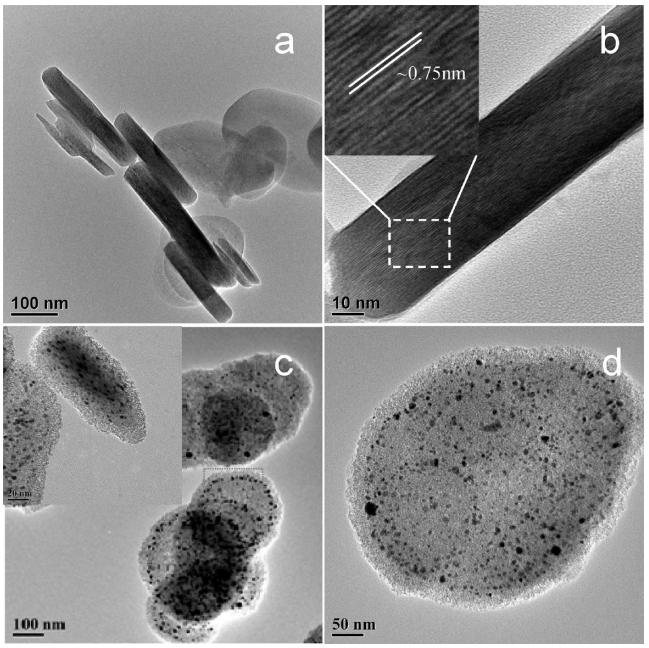

Figure 2. TEM images of LDH-CO_3^{2-} (a,b) and AAMO/Au/$mSiO_2$ (c,d). The inset in (c) is the TEM image of an AAMO/Au/$mSiO_2$ particle with the electron beam parallel to the plate surface (scale bar: 20 nm).

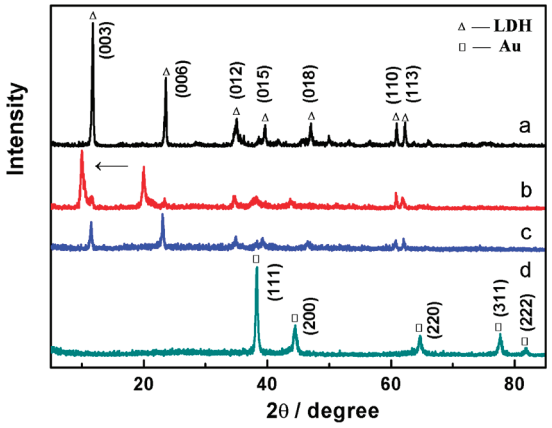

Figure 3. Powder XRD patterns of LDH-CO_3^{2-} (a), LDH-NO_3^{2-} (b), LDH/Au$(OH)_3$ (c), and AAMO/Au/$mSiO_2$ (d).

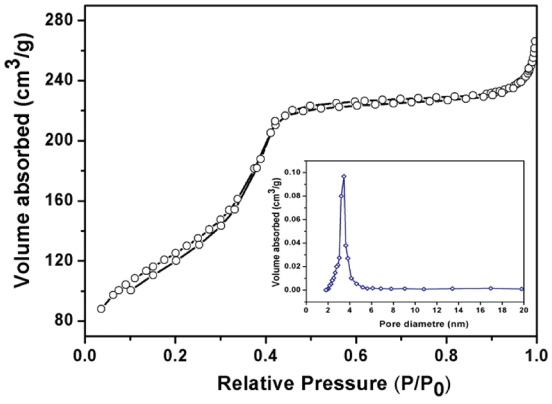

Figure 4. N_2 adsorption−desorption isotherms and the corresponding BJH pore size distribution of AAMO/Au/$mSiO_2$ composite.

basal spacing of 7.5 Å, which is consistent with the results from the HRTEM images (Figure 2b). A new series of intense basal reflections at lower 2θ angles appear in Figure 3b and the (001) basal spacing of the LDH increases from 0.75 to 0.88 nm, suggesting that the successful decarbonation and the incorporation of NO_3^{2-}. There are still typical but ultraweak diffraction peaks of LDH-CO_3^{2-} coexisting with those of LDH-NO_3^{2-}, demonstrating a small amount of residual CO_3^{2-} in the obtained LDH-NO_3^{2-}. After the deposition of amorphous Au$(OH)_3$ on the surface of LDH, the diffraction peak positions shift again toward higher angles (Figure 3c), and the (001) basal spacing is 0.77 nm, implying that Cl^- ions, coming from $HAuCl_4$ at pH = 8.0,[44,45] have been incorporated in the LDH.[46,47] Typical Au $Fm\bar{3}m$ crystal structure can be found in Figure 3d, which can be indexed to the (111), (200), (220), (311), and (222) planes, showing the formation of AAMO/Au/$mSiO_2$ composite. The calculated basal spacing of (111) plane of Au is 0.23 nm from the pattern, which is consistent with HRTEM image of gold nanoparticles in Figure S2a. The diffraction peaks typical for LDH disappeared without an indication of any new crystallized compound, which demonstrates that layer-structured LDH has changed to the amorphous substance AAMO by decomposition during heat treatment. The average diameter of Au NPs in AAMO/Au/$mSiO_2$ composite is around 5.8 nm (Figure S2b), and a considerable amount of isolated Au NPs distributed at the interface between AAMO core and $mSiO_2$ shell (Figure 2c,d), which would allow rapid access of reactants from outside. Figure 4 gives the nitrogen adsorption/desorption isotherms and the corresponding BJH pore size distribution of AAMO/Au/$mSiO_2$. The obvious rise between P/P_o = 0.2−0.4 indicates the presence of mesopores in the composite. The specific surface area, pore volume, and the most probable pore diameter were calculated to be 456 m^2/g, 0.43 cm^3/g, and 3.5 nm, respectively. The content of Au in AAMO/Au/$mSiO_2$ is 16.2%, as measured by inductively coupled plasma (ICP)-atomic emission spectroscopy analysis.

The amorphous AAMO core in AAMO/Au/$mSiO_2$ composite, which was a result of the collapse of layered LDH structure during calcination accompanying the formation of highly dispersed Au NPs, is essential in preventing Au NPs from accumulation/aggregation between each other through fixing them at interface between AAMO core and mesoporous SiO_2 shell. The Au NPs, at the inner pore mouths of the $mSiO_2$ shell, could allow the fast access of reactants from the outside of particles through the mesoporous channels of the protective mesoporous silica shell. Figure S3a,b shows that the Au NPs in one mesoporous shell would aggregate and grow into one large particle if AAMO was removed from AAMO/Au/$mSiO_2$ composite by acid corrosion. The $mSiO_2$ shell of 25−30 nm in thickness provided diffusion pathways for both reactants and product of limited molecular size, and also prevented Au NPs from migration and contact with each other on the surface of AAMO to form aggregates and/or grow into large particles. There are no Au NPs observable in the channel of mesoporous shell, revealing that the mesoporous shell is an effective pathway for the free diffusion of reactants and products. Figure S3c−f shows the TEM images of AAMO/Au without an $mSiO_2$ capping layer obtained by calcining LDH-Au$(OH)_3$ directly. Au NPs with a much larger diameter in AAMO/Au than that in AAMO/Au/$mSiO_2$ were found, which meant that the migration and aggregation of Au NPs on the surface of AAMO would take place to a large extent during synthesis. A

dx.doi.org/10.1021/la2045898 | Langmuir 2012, 28, 4920−4925

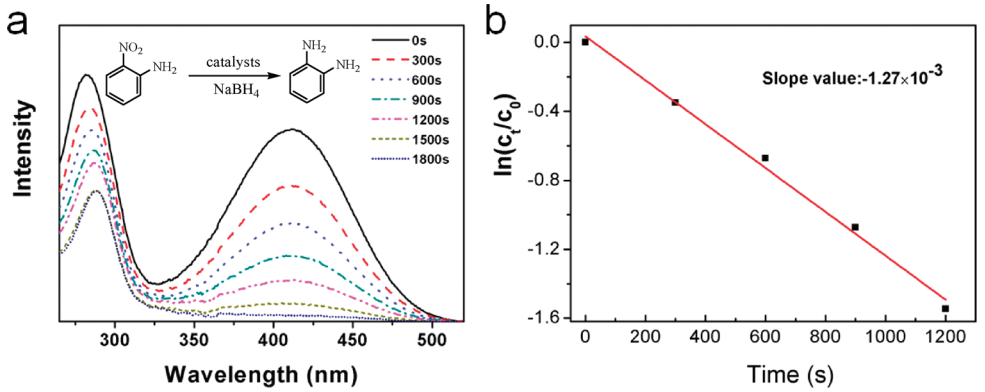

Figure 5. (a) UV–vis spectra of the reaction mixture (5 mL 0.1 M $NaBH_4$ and 10 mL 6×10^{-3} M 2-nitroaniline) of different reaction times catalyzed by 2 mg AAMO/Au/$mSiO_2$. (b) Plot of $\ln(C_t/C_0)$ vs time using AAMO/Au/$mSiO_2$ as catalyst.

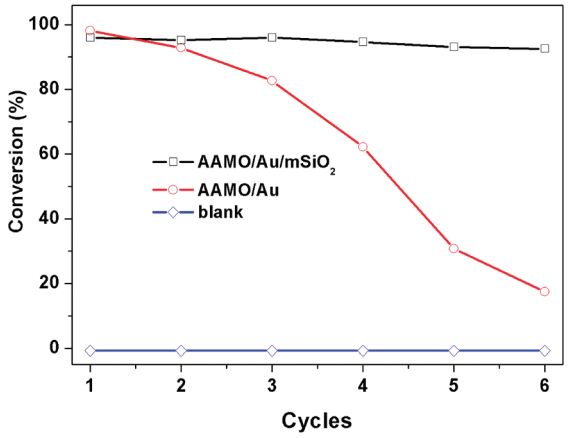

Figure 6. Conversion of 2-nitroaniline in 6 successive cycles of reduction with AAMO/Au/$mSiO_2$ and AAMO/Au without $mSiO_2$ capping layers as catalysts, respectively.

possible mechanism for that was described as follows: the Au NPs have a lower melting point compared with bulk Au; therefore, the initial NPs with a very small diameter would be in a melted form during calcination.[48] So, they are almost free to migrate, come in contact with each other, and form aggregates in the preparation of AAMO/Au. Comparatively, the mesoporous silica shell could provide a space barrier to prevent Au NPs from migration and agglomeration with each other to a large extent, and therefore, the diameter of Au NPs in AAMO/Au/$mSiO_2$ is significantly smaller than that in AAMO/Au. In addition, the Au NPs were mainly located on the surface of AAMO in AAMO/Au composite, which meant that the Au NPs tended to nucleate and grow on the surface of AAMO during synthesis, and also implied that, before calcining AAMO/$Au(OH)_3$, the $Au(OH)_3$ was mainly on the surface of the LDH particles.

A 2-nitroaniline reduction reaction was carried out to evaluate the catalytic performance of sample AAMO/Au/$mSiO_2$.[19] A catalyst/reactant (5 mg m-n-e Au core/MSS/10 mL 6×10^{-3} M 2-nitroaniline) mass ratio of 0.24 was adopted. Figure 5a demonstrates the intensity change of the 410 nm peak with reaction time. The continuing decrease of the 410 nm peak intensity with time reflects continuing conversion of the reactant, which can be used to calculate the reaction rate constant. The parameters of C_t and C_0, the 2-nitroaniline concentrations at time t and 0, respectively, were measured from the relative intensities of the corresponding absorbances, A_t/A_0. A linear relation of $\ln(C_t/C_0)$ versus time was then obtained, indicating that the reaction followed diffusion-coupled first-order reaction kinetics.[14] The rate constant was estimated to be 1.27×10^{-3} from the line slope in Figure 5b.

In order to demonstrate the stability of Au NPs in AAMO/Au/$mSiO_2$ system against coalescence, 6 successive cycles of reaction were performed using the same procedures as reported in the literature[17] with a higher catalyst/reactant mass ratio of 1.20. The reaction did not take place under the absence of catalysts as reported in the literature.[19] AAMO/Au/$mSiO_2$ showed excellent stability in the reaction and the conversion of 2-nitroaniline for all cycles exceeded 90% in 15 min, while the conversion using AAMO/Au as a catalyst showed a quick decline from the second cycle (Figure 6), which was most

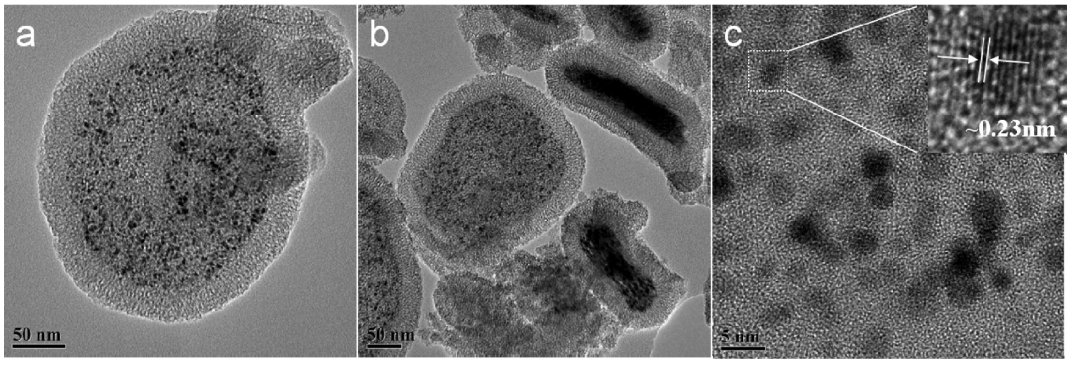

Figure 7. TEM (a,b) and HRTEM (c) images of the prepared AAMO/Pt/$mSiO_2$.

dx.doi.org/10.1021/la2045898 | Langmuir 2012, 28, 4920–4925

probably due to the agglomeration/growth of the bare Au NPs located at the surface of AAMO particles without the protection from the $mSiO_2$ shell.

In addition to AAMO/Au/$mSiO_2$, AAMO/Pt/$mSiO_2$ was also fabricated using the same method. Figure 7 is TEM images of synthesized AAMO/Pt/$mSiO_2$. The Pt NPs embedded in the AAMO cores are 3.2 nm in diameter. This method is expected to be extendible to synthesis of other kinds of similar metal-based catalytic systems.

CONCLUSION

In summary, we have demonstrated the successful fabrication of AAMO/Au/$mSiO_2$ composite. The AAMO core is an essential support to disperse and fix Au NPs at the interface between the core and mesoporous SiO_2 shell, and the mesoporous shell provides the diffusion channels for reactants and products, which allows efficient access of reactants to the catalytic NPs. Au NPs with an average diameter of 5.8 nm, located at the inner pore mouths of $mSiO_2$ shell, exhibit favorable catalytic activity and reusability in the 2-nitroaniline reduction. This method is expected to fabricate a variety of multinanoparticle-embedded core/$mSiO_2$ shell structured composites.

ASSOCIATED CONTENT

Supporting Information

Additional figures. This material is available free of charge via the Internet at http://pubs.acs.org.

AUTHOR INFORMATION

Corresponding Author

*E-mail: jlshi@sunm.shcnc.ac.cn. Fax: (+) 86-21-52413122. Tel: (+) 86-21-52412712.

Notes

The authors declare no competing financial interest.

ACKNOWLEDGMENTS

This work was supported by National Natural Science Foundation of China (Grant Nos. 50823007 and 50872140).

REFERENCES

(1) Garcia-Martinez, J. C.; Lezutekong, R.; Crooks, R. M. Dendrimer-encapsulated Pd nanoparticles as aqueous, room-temperature catalysts for the Stille reaction. *J. Am. Chem. Soc.* **2005**, *127*, 5097−5103.

(2) Son, S. U.; Jang, Y.; Yoon, K. Y.; Kang, E.; Hyeon, T. Facile synthesis of various phosphine-stabilized monodisperse palladium nanoparticles through the understanding of coordination chemistry of the nanoparticles. *Nano Lett.* **2004**, *4*, 1147−1151.

(3) Narayanan, R.; El-Sayed, M. A. Changing catalytic activity during colloidal platinum nanocatalysis due to shape changes: Electron-transfer reaction. *J. Am. Chem. Soc.* **2004**, *126*, 7194−7195.

(4) Roucoux, A.; Schulz, J.; Patin, H. Reduced transition metal colloids: A novel family of reusable catalysts? *Chem. Rev.* **2002**, *102*, 3757−3778.

(5) Tsunoyama, H.; Sakurai, H.; Negishi, Y.; Tsukuda, T. Size-specific catalytic activity of polymer-stabilized gold nanoclusters for aerobic alcohol oxidation in water. *J. Am. Chem. Soc.* **2005**, *127*, 9374−9375.

(6) Jana, N. R.; Peng, X. G. Single-phase and gram-scale routes toward nearly monodisperse Au and other noble metal nanocrystals. *J. Am. Chem. Soc.* **2003**, *125*, 14280−14281.

(7) Zhou, H. P.; Wu, H. S.; Shen, J.; Yin, A. X.; Sun, L. D.; Yan, C. H. Thermally Stable Pt/CeO2 Hetero-Nanocomposites with High Catalytic Activity. *J. Am. Chem. Soc.* **2010**, *132*, 4998−4999.

(8) Joo, S. H.; Park, J. Y.; Tsung, C. K.; Yamada, Y.; Yang, P. D.; Somorjai, G. A. Thermally stable Pt/mesoporous silica core-shell nanocatalysts for high-temperature reactions. *Nat. Mater.* **2009**, *8*, 126−131.

(9) Ikeda, S.; Ishino, S.; Harada, T.; Okamoto, N.; Sakata, T.; Mori, H.; Kuwabata, S.; Torimoto, T.; Matsumura, M. Ligand-free platinum nanoparticles encapsulated in a hollow porous carbon shell as a highly active heterogeneous hydrogenation catalyst. *Angew. Chem., Int. Ed.* **2006**, *45*, 7063−7066.

(10) Shi, J. L.; Hua, Z. L.; Zhang, L. X. Nanocomposites from ordered mesoporous materials. *J. Mater. Chem.* **2004**, *14*, 795−806.

(11) Wu, P. P.; Bai, P.; Loh, K. P.; Zhao, X. S. Au nanoparticles dispersed on functionalized mesoporous silica for selective oxidation of cyclohexane. *Catal. Today* **2010**, *158*, 220−227.

(12) Besson, E.; Mehdi, A.; Reye, C.; Corriu, R. J. P. Soft route for monodisperse gold nanoparticles confined within SH-functionalized walls of mesoporous silica. *J. Mater. Chem.* **2009**, *19*, 4746−4752.

(13) Zhao, Y.; Jiang, L. Hollow Micro/Nanomaterials with Multilevel Interior Structures. *Adv. Mater.* **2009**, *21*, 3621−3638.

(14) Lee, J.; Park, J. C.; Song, H. A nanoreactor framework of a Au@SiO2 yolk/shell structure for catalytic reduction of p-nitrophenol. *Adv. Mater.* **2008**, *20*, 1523−1528.

(15) Han, L.; Wei, H.; Tu, B.; Zhao, D. Y. A facile one-pot synthesis of uniform core-shell silver nanoparticle@mesoporous silica nanospheres. *Chem. Commun.* **2011**, *47*, 8536−8538.

(16) Wang, H. Y.; Wu, D. Y.; Li, D. Z.; Niu, Z. W.; Chen, Y. Z.; Tang, D. H.; Wu, M.; Cao, J. H.; Huang, Y. Fabrication of continuous highly ordered mesoporous silica nanofibre with core/sheath structure and its application as catalyst carrier. *Nanoscale* **2011**, *3*, 3601−3604.

(17) Zhang, Q.; Zhang, T. R.; Ge, J. P.; Yin, Y. D. Permeable silica shell through surface-protected etching. *Nano Lett.* **2008**, *8*, 2867−2871.

(18) Lou, X. W.; Archer, L. A.; Yang, Z. C. Hollow Micro-/Nanostructures: Synthesis and Applications. *Adv. Mater.* **2008**, *20*, 3987−4019.

(19) Tan, L. F.; Chen, D.; Liu, H. Y.; Tang, F. Q. A Silica Nanorattle with a Mesoporous Shell: An Ideal Nanoreactor for the Preparation of Tunable Gold Cores. *Adv. Mater.* **2010**, *22*, 4885−4889.

(20) Huang, X. Q.; Guo, C. Y.; Zuo, L. Q.; Zheng, N. F.; Stucky, G. D. An Assembly Route to Inorganic Catalytic Nanoreactors Containing Sub-10-nm Gold Nanoparticles with Anti-Aggregation Properties. *Small* **2009**, *5*, 361−365.

(21) Park, J. N.; Forman, A. J.; Tang, W.; Cheng, J. H.; Hu, Y. S.; Lin, H. F.; McFarland, E. W. Highly Active and Sinter-Resistant Pd-Nanoparticle Catalysts Encapsulated in Silica. *Small* **2008**, *4*, 1694−1697.

(22) Kamata, K.; Lu, Y.; Xia, Y. N. Synthesis and characterization of monodispersed core-shell spherical colloids with movable cores. *J. Am. Chem. Soc.* **2003**, *125*, 2384−2385.

(23) Lee, J.; Park, J. C.; Bang, J. U.; Song, H. Precise tuning of porosity and surface functionality in Au@SiO2 nanoreactors for high catalytic efficiency. *Chem. Mater.* **2008**, *20*, 5839−5844.

(24) Roca, M.; Haes, A. J. Silica-Void-Gold Nanoparticles: Temporally Stable Surf ace-Enhanced Raman Scattering Substrates. *J. Am. Chem. Soc.* **2008**, *130*, 14273−14279.

(25) Kim, M.; Sohn, K.; Bin Na, H.; Hyeon, T. Synthesis of nanorattles composed of gold nanoparticles encapsulated in mesoporous carbon and polymer shells. *Nano Lett.* **2002**, *2*, 1383−1387.

(26) Wang, Y. F.; Biradar, A. V.; Duncan, C. T.; Asefa, T. Silica nanosphere-supported shaped Pd nanoparticles encapsulated with nanoporous silica shell: Efficient and recyclable nanocatalysts. *J. Mater. Chem.* **2010**, *20*, 7834−7841.

(27) Kumagi, H.; Yano, K. Synthesis and Characterization of Au-Loaded Core/Shell Mesoporous Silica Spheres Containing Propyl Group in the Shell. *Chem. Mater.* **2010**, *22*, 5112−5118.

(28) Dai, Y. Q.; Lim, B.; Yang, Y.; Cobley, C. M.; Li, W. Y.; Cho, E. C.; Grayson, B.; Fanson, P. T.; Campbell, C. T.; Sun, Y. M.; Xia, Y. N. A Sinter-Resistant Catalytic System Based on Platinum Nanoparticles

Supported on TiO(2) Nanofibers and Covered by Porous Silica. *Angew. Chem., Int. Ed.* **2010**, *49*, 8165−8168.
(29) Darder, M.; Lopez-Blanco, M.; Aranda, P.; Leroux, F.; Ruiz-Hitzky, E. Bio-nanocomposites based on layered double hydroxides. *Chem. Mater.* **2005**, *17*, 1969−1977.
(30) Choy, J. H.; Oh, J. M.; Park, M.; Sohn, K. M.; Kim, J. W. Inorganic-biomolecular hybrid nanomaterials as a genetic molecular code system. *Adv. Mater.* **2004**, *16*, 1181−1184.
(31) Yan, D. P.; Lu, J.; Wei, M.; Qin, S. H.; Chen, L.; Zhang, S. T.; Evans, D. G.; Duan, X. Heterogeneous Transparent Ultrathin Films with Tunable-Color Luminescence Based on the Assembly of Photoactive Organic Molecules and Layered Double Hydroxides. *Adv. Funct. Mater.* **2011**, *21*, 2497−2505.
(32) Shi, W. Y.; Ji, X. L.; Zhang, S. T.; Wei, M.; Evans, D. G.; Duan, X. Fluorescence Chemosensory Ultrathin Films for Cd(2+) Based on the Assembly of Benzothiazole and Layered Double Hydroxide. *J. Phys. Chem. C* **2011**, *115*, 20433−20441.
(33) Liu, J.; Harrison, R.; Zhou, J. Z.; Liu, T. T.; Yu, C. Z.; Lu, G. Q.; Qiao, S. Z.; Xu, Z. P. Synthesis of nanorattles with layered double hydroxide core and mesoporous silica shell as delivery vehicles. *J. Mater. Chem.* **2011**, *21*, 10641−10644.
(34) Bao, H. F.; Yang, J. P.; Huang, Y.; Xu, Z. P.; Hao, N.; Wu, Z. X.; Lu, G. Q.; Zhao, D. Y. Synthesis of well-dispersed layered double hydroxide core@ordered mesoporous silica shell nanostructure (LDH@mSiO(2)) and its application in drug delivery. *Nanoscale* **2011**, *3*, 4069−4073.
(35) Beaudot, P.; De Roy, M. E.; Besse, J. P. Intercalation of noble metal complexes in LDH compounds. *J. Solid. State. Chem.* **2004**, *177*, 2691−2698.
(36) Wang, L.; Zhang, J.; Meng, X. J.; Zheng, D. F.; Xiao, F. S. Superior catalytic properties in aerobic oxidation of alcohols over Au nanoparticles supported on layered double hydroxide. *Catal. Today* **2011**, *175*, 404−410.
(37) Singha, S.; Sahoo, M.; Parida, K. M. Highly active Pd nanoparticles dispersed on amine functionalized layered double hydroxide for Suzuki coupling reaction. *Dalton. T.* **2011**, *40*, 7130−7132.
(38) Mi, F.; Chen, X. T.; Ma, Y. W.; Yin, S. T.; Yuan, F. L.; Zhang, H. Facile synthesis of hierarchical core-shell Fe(3)O(4)@MgAl-LDH@Au as magnetically recyclable catalysts for catalytic oxidation of alcohols. *Chem. Commun.* **2011**, *47*, 12804−12806.
(39) Chen, C. P.; Gunawan, P.; Xu, R. Self-assembled Fe(3)O(4)-layered double hydroxide colloidal nanohybrids with excellent performance for treatment of organic dyes in water. *J. Mater. Chem.* **2011**, *21*, 1218−1225.
(40) Oh, J. M.; Choi, S. J.; Lee, G. E.; Han, S. H.; Choy, J. H. Inorganic Drug-Delivery Nanovehicle Conjugated with Cancer-Cell-Specific Ligand. *Adv. Funct. Mater.* **2009**, *19*, 1617−1624.
(41) Liu, S. S.; Chen, H. M.; Lu, X. H.; Deng, C. H.; Zhang, X. M.; Yang, P. Y. Facile Synthesis of Copper(II)Immobilized on Magnetic Mesoporous Silica Microspheres for Selective Enrichment of Peptides for Mass Spectrometry Analysis. *Angew. Chem., Int. Ed.* **2010**, *49*, 7557−7561.
(42) Ding, K. L.; Hu, B. J.; Xie, Y.; An, G. M.; Tao, R. T.; Zhang, H. Y.; Liu, Z. M. A simple route to coat mesoporous SiO2 layer on carbon nanotubes. *J. Mater. Chem.* **2009**, *19*, 3725−3731.
(43) Iyi, N.; Matsumoto, T.; Kaneko, Y.; Kitamura, K. Deintercalation of carbonate ions from a hydrotalcite-like compound: Enhanced decarbonation using acid-salt mixed solution. *Chem. Mater.* **2004**, *16*, 2926−2932.
(44) Grisel, R. J. H.; Kooyman, P. J.; Nieuwenhuys, B. E. Influence of the preparation of Au/Al2O3 on CH4 oxidation activity. *J. Catal.* **2000**, *191*, 430−437.
(45) Moreau, F.; Bond, G. C.; Taylor, A. O. Gold on titania catalysts for the oxidation of carbon monoxide: control of pH during preparation with various gold contents. *J. Catal.* **2005**, *231*, 105−114.
(46) Liu, Z. P.; Ma, R. Z.; Osada, M.; Iyi, N.; Ebina, Y.; Takada, K.; Sasaki, T. Synthesis, anion exchange, and delamination of Co-Al layered double hydroxide: Assembly of the exfoliated nanosheet/polyanion composite films and magneto-optical studies. *J. Am. Chem. Soc.* **2006**, *128*, 4872−4880.
(47) Okamoto, K.; Sasaki, T.; Fujita, T.; Iyi, N. Preparation of highly oriented organic-LDH hybrid films by combining the decarbonation, anion-exchange, and delamination processes. *J. Mater. Chem.* **2006**, *16*, 1608−1616.
(48) Nanda, K. K.; Sahu, S. N.; Behera, S. N. Liquid-drop model for the size-dependent melting of low-dimensional systems. *Phys. Rev. A* **2002**, *66*, 013208.